

Supplementary Materials for

Programmable colloidal molecules from sequential capillarity-assisted particle assembly

Songbo Ni, Jessica Leemann, Ivo Buttinoni, Lucio Isa, Heiko Wolf

Published 1 April 2016, *Sci. Adv.* **2**, e1501779 (2016)

DOI: 10.1126/sciadv.1501779

This PDF file includes:

- Technical details of the assembly of linear colloidal chains.
- Technical details of the assembly of nonlinear colloidal clusters (trimers and 3D clusters).
- Fig. S1. SEM images of different colloidal chains on the template.
- Fig. S2. Effect of trap size on the assembly yield of R-G-B PS trimers.
- Fig. S3. Yield of assembled carboxylate PS and amine PS dumbbells on an area of $5 \times 12 \text{ mm}^2$.
- Fig. S4. EDX spectroscopy of three-particle chains with plain SiO_2 , PS, and magnetic SiO_2 .
- Fig. S5. Linking of clusters by thermal sintering.
- Fig. S6. Harvesting of clusters.
- Fig. S7. Harvesting of clusters at extremely low temperatures.
- Fig. S8. Effects of varying lateral trap dimensions on the structure of 3D clusters.
- Fig. S9. Effects of local assembly direction on the first sCAPA step of colloidal trimers.
- Fig. S10. Effects of local assembly direction on the assembly of open colloidal trimers with three different lobes.
- Legends for movies S1 to S9

Other Supplementary Material for this manuscript includes the following:

(available at advances.sciencemag.org/cgi/content/full/2/4/e1501779/DC1)

- Movie S1 (.avi format). The first assembly step for the fabrication of surfactant-like colloidal chains.

- Movie S2 (.avi format). The second assembly step for the fabrication of surfactant-like colloidal chains.
- Movie S3 (.avi format). Brownian motion of a dumbbell with a magnetic head and a PS lobe dispersed in water after harvesting.
- Movie S4 (.avi format). Brownian motion of a four-particle chain with a magnetic head and a PS tail dispersed in water after harvesting.
- Movie S5 (.avi format). Brownian motion of an eight-particle chain with a magnetic head and a PS tail dispersed in water after harvesting.
- Movie S6 (.avi format). Rotation of colloidal chains with a magnetic head in an external rotating magnetic field.
- Movie S7 (.avi format). Oscillation of colloidal chains with a magnetic head in an external oscillating magnetic field.
- Movie S8 (.avi format). Translation of a colloidal chain with a magnetic head by a permanent magnet.
- Movie S9 (.avi format). The third assembly step for the fabrication of open PS trimers with three different lobes.

Supplementary Materials

Technical details of the assembly of linear colloidal chains

In addition to the depth of the trap and the surface tension (25), two other parameters can influence the assembly of linear colloidal chains resulting from sCAPA: the lateral trap dimensions and the local assembly direction. The width of the trap determines the bond angle between adjacent particles.

Narrower traps force particles into a tight, single file, whereas wider traps allow zig-zag assemblies with defined bond angles (16). The length of the trap defines the maximum possible length of the linear colloidal chains. The direction in which the meniscus moves relative to the trap is not very important for the assembly of single particles. This is confirmed by the assembly of the barcode and block copolymer colloidal chains, where trap orientations of up to 45° relative to the direction of meniscus movement do not affect the selectivity of the assembly. An angle of more than 45° implies that the meniscus actually sweeps along the short axis of the trap, leading to the assembly of multiple particles simultaneously.

Therefore, in the assembly of surfactant-like colloidal chains, the two steps have different requirements in relation to the trap orientation as reported in the main text.

Technical details of the assembly of nonlinear colloidal clusters (trimers and 3D clusters)

Similarly, the lateral dimensions of the trap and the local assembly direction are the two key parameters to control the assembly of nonlinear clusters. The lateral size of the trap controls the yield of the assembled trimers as discussed in the main text. For planar trimers, the orientation of the traps is such that in each step the meniscus moves macroscopically to a predefined corner in the triangular trap. In the first step, a slight shift of the local assembly direction relative to the bisector of the predefined corner is maintained, favoring the assembly of only one particle into that corner. In contrast, when the meniscus moves straight along the bisector of the predefined corner, it is probable that two particles, or even three, are trapped simultaneously (fig. S9A). This results from the fact that if two particles move forward together, they may get stuck on the two sides of the trap simultaneously, which prevents them from moving further and occasionally even may lead to the trapping of a third particle. If the assembly

direction shifts too much (e.g., as for the shift in fig. S9B), two particles may be assembled along the side towards which the meniscus moves. Therefore, in the first assembly step, a small shift of the assembly direction away from the bisector of the predefined corner ($\sim 15 - 45^\circ$) is needed to trap one particle selectively in each corner. In the case of the closed trimers, the second and third steps are significantly less sensitive to the assembly direction, given the different geometry of the already partially filled traps, which easily guides the rest of the sequential filling. In the assembly of separated trimers, however, care needs to be taken in each step to prevent particles from assembling towards the corner that has already been filled (See fig. S10A, B and Movie S9). Further details on the mechanisms and forces at play during sCAPA can be found in Ref. 25.

In the assembly of 3D clusters, the vertical position of the fourth particle depends on arrangement of the three previously deposited particles, i.e., on the space left in the center of the separated trimers, and thus on the lateral trap size. Figure S8A shows the variation of the available space for the fourth particle in the separated trimers, and fig. S8C and D demonstrate the variation in the vertical position.

Supplementary figures

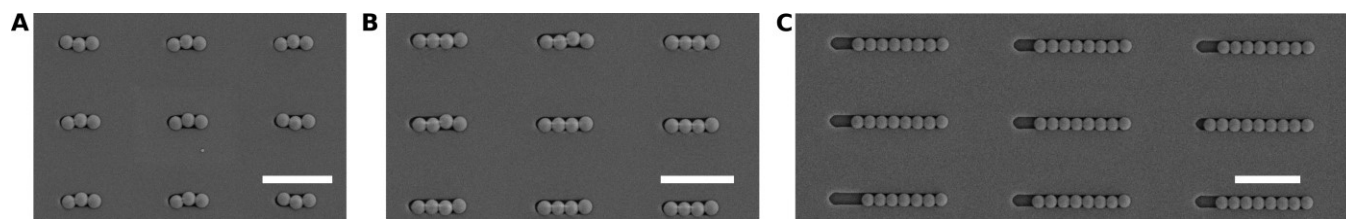


fig. S1. SEM images of different colloidal chains on the template. (A) G-R-B three-particle PS chains. (B) B-G-R-B four-particle PS chains. (C) Surfactant-like colloidal chains with a red PS particle in the front followed by a tail of green PS particles.

All scale bars are 5 μm .

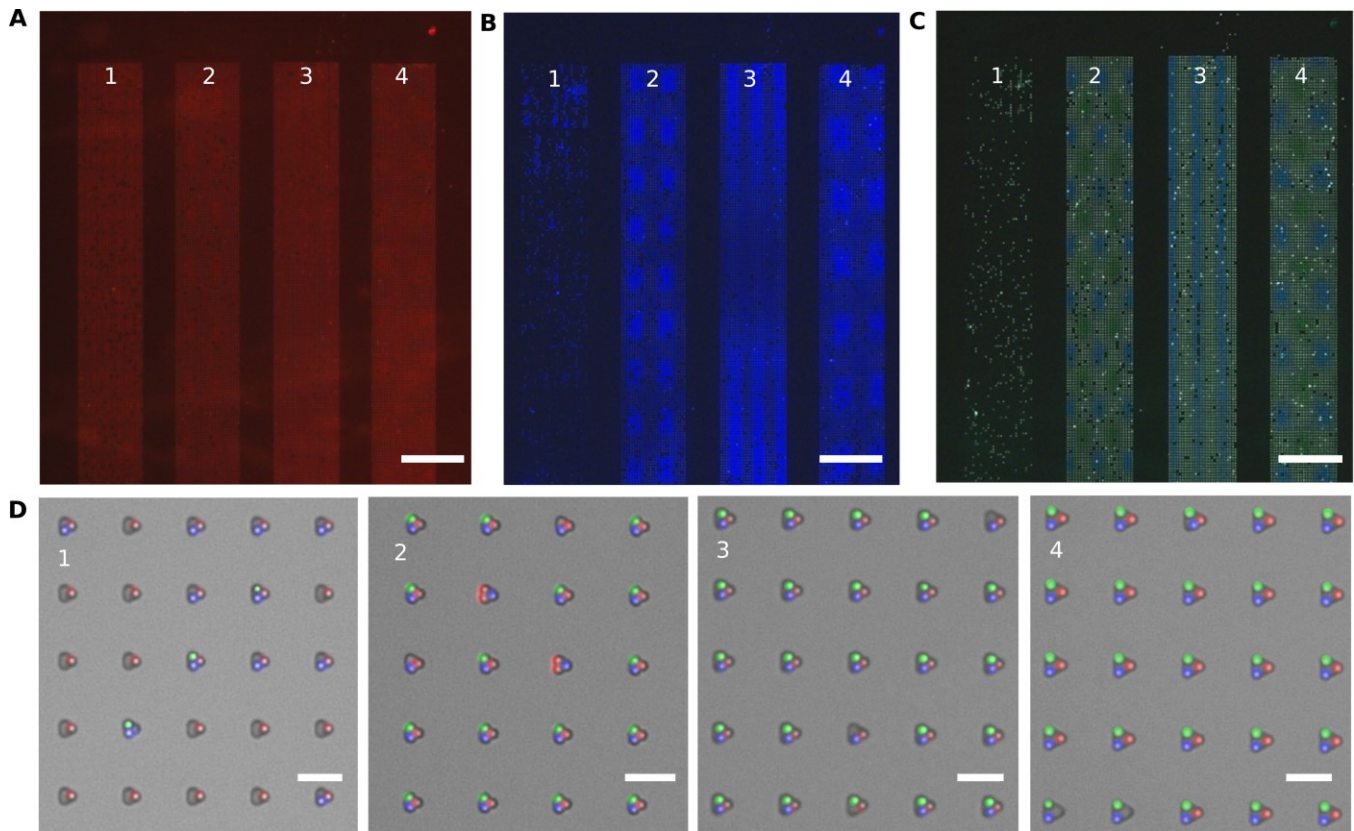


fig. S2. Effect of trap size on the assembly yield of R-G-B PS trimers. (A to C) Overview images of the template using different fluorescence channels. Four stripes (1 to 4) are shown, with the size of the individual trap increasing from left to right. The sizes of the traps in each stripe are given in the SEM images in Fig. 4C. Red particles are assembled first, followed by the blue and green particles. The scale bars are 200 μm . (D) Zooms of the individual stripes (overlays of fluorescence and bright-field images) showing the particle assembly in the differently sized traps. The numbers on the top left correspond to the number of the stripe labeled in A, B and C. The scale bars are 5 μm .

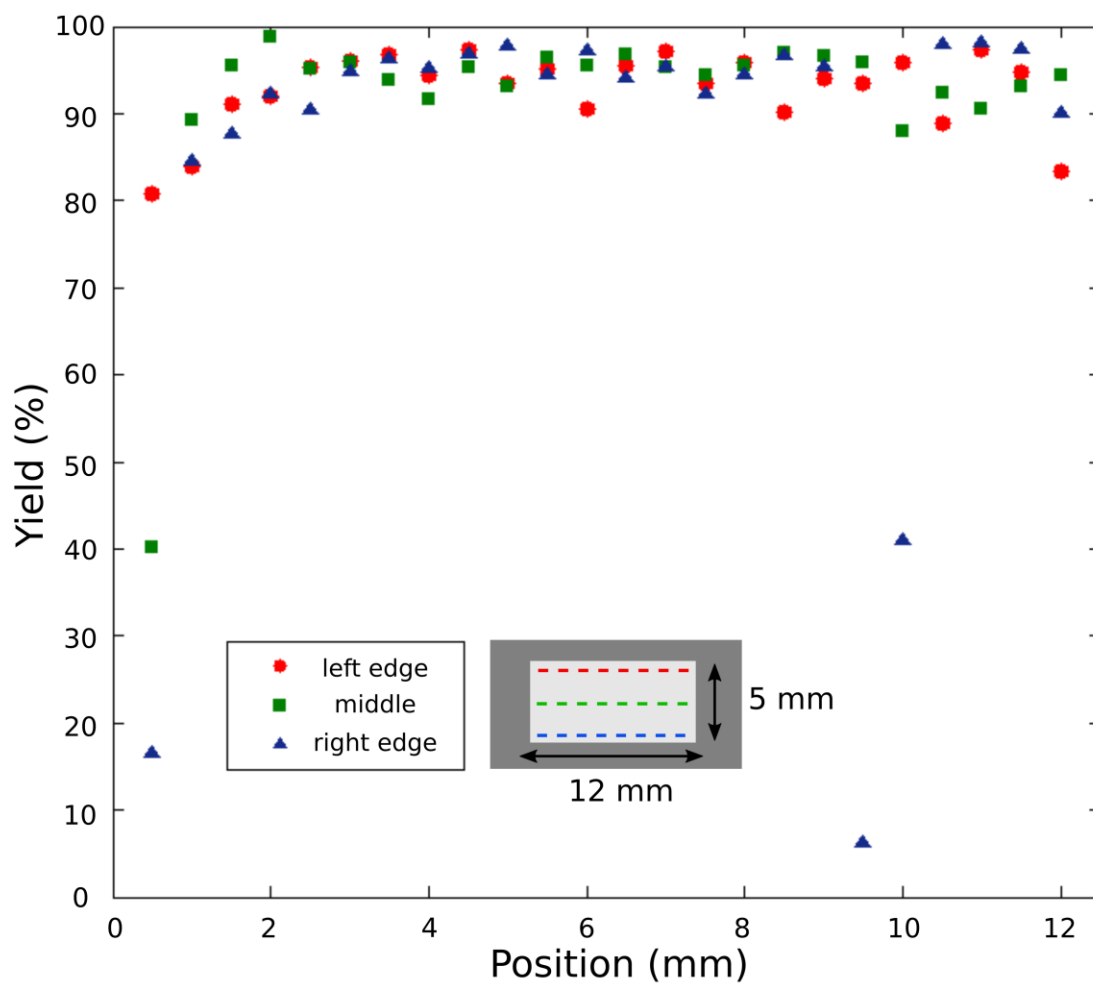


fig. S3. Yield of assembled carboxylate PS and amine PS dumbbells on an area of $5 \times 12 \text{ mm}^2$. Data collected along three different lines (edges and center of the template, schematically shown in the inset). Sporadic low-yield spikes are observed at the beginning of the assembly when the accumulation zone is not fully developed and later in the assembly where larger agglomerates disturb the deposition process.

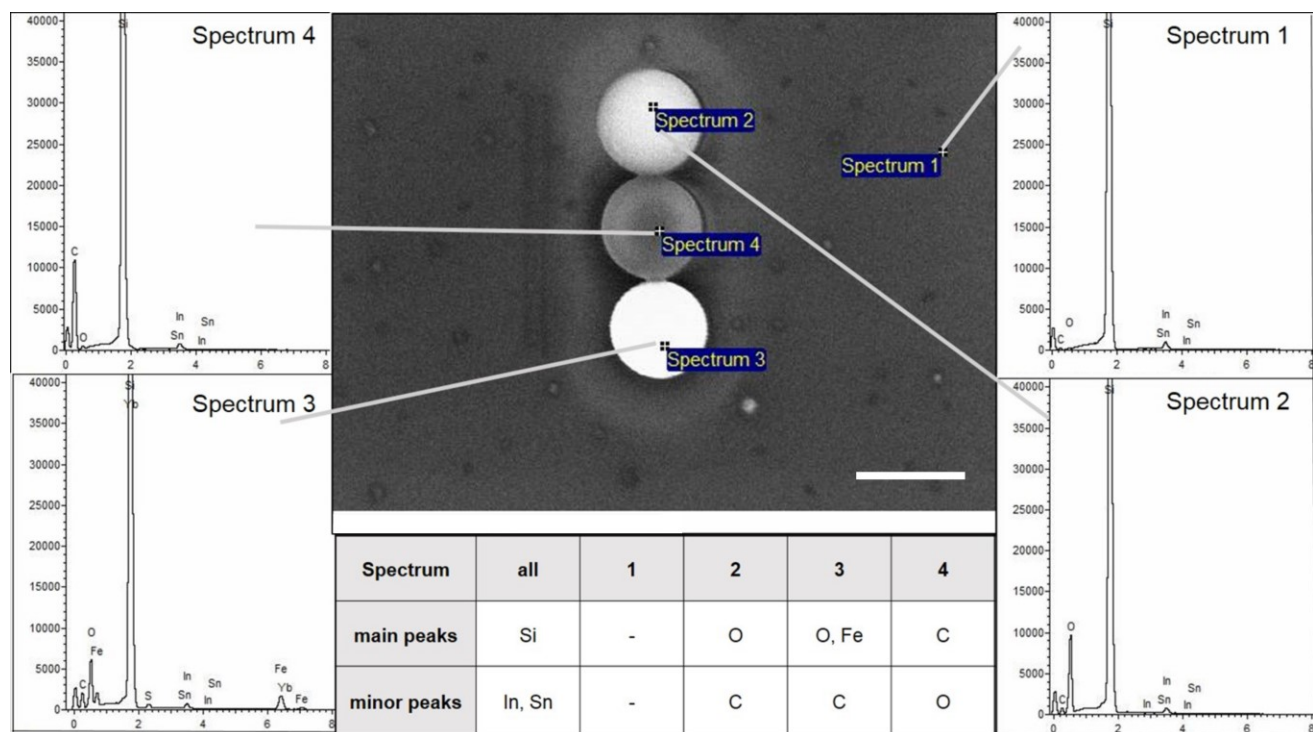


fig. S4. EDX spectroscopy of three-particle chains with plain SiO_2 (top), PS (middle), and magnetic SiO_2 (bottom). The scale bar is 1 μm . The spectra confirm that the composition of the chains follows the programmed sequence.

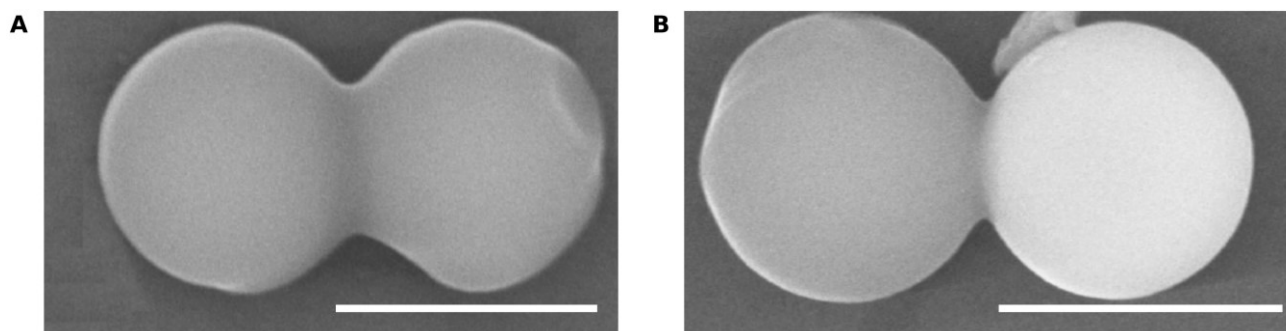


fig. S5. Linking of clusters by thermal sintering. (A) SEM image of a linked PS dumbbell. (B) SEM image of a linked PS and SiO_2 dumbbell. The scale bars are 1 μm .

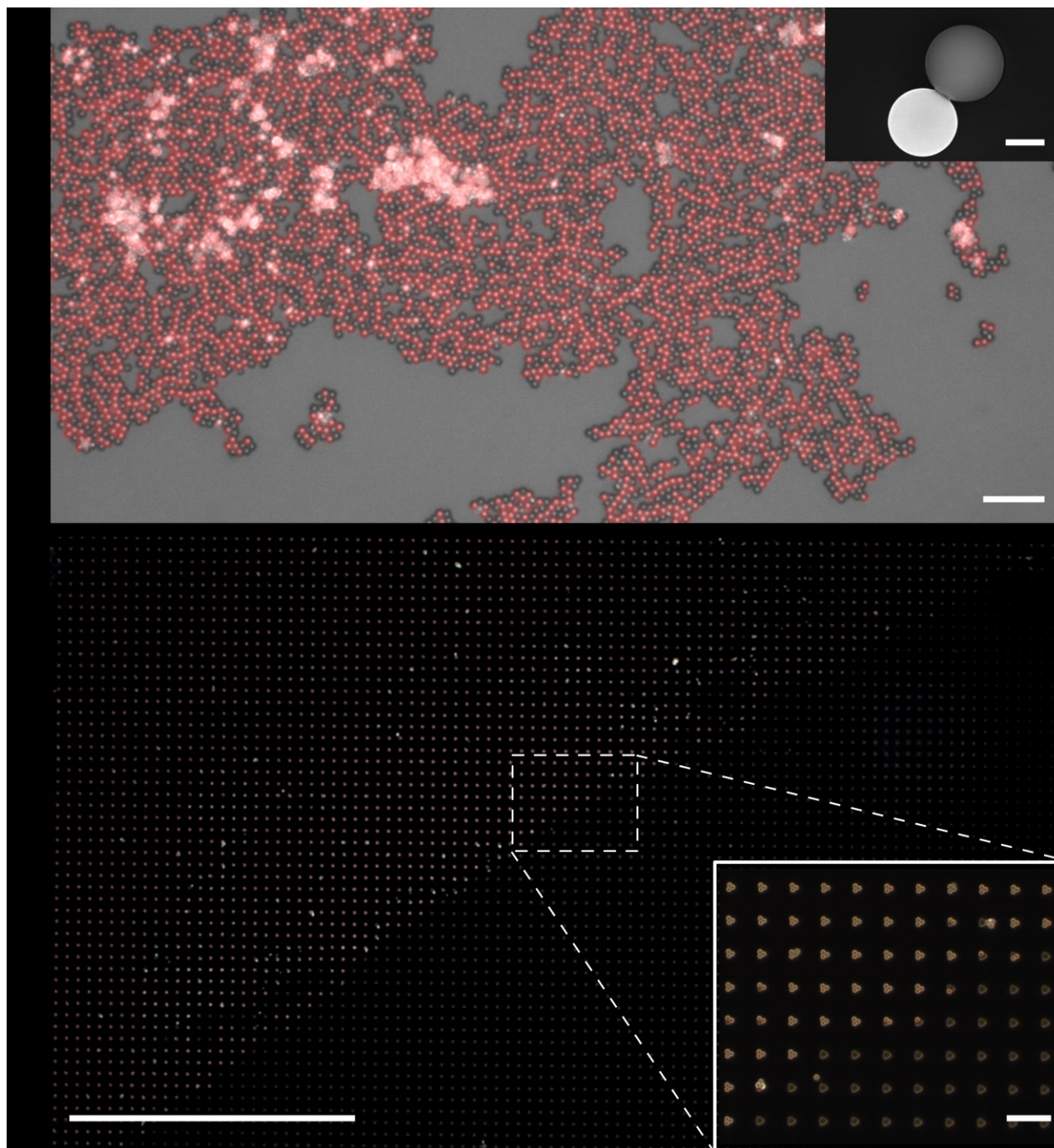


fig. S6. Harvesting of clusters. (A) Large-scale image of PS-magnetic silica dumbbells dried on a substrate after harvesting and dispersion in water (overlay of fluorescence and bright-field image). Scale bar: 10 μm . Inset: SEM image of the dumbbells. Scale bar: 500 nm. (B) During the harvesting process, the particles covered by the drop are transferred with a yield close to 100% (usually a sharp boundary at the drop is seen — evidence of the high transfer efficiency). Dark-field microscopy image of a template with triangular traps after harvesting showing a sharp boundary between the harvested and non-harvested regions where the droplet was placed on the substrate. Scale bar: 200 μm . The inset shows the details of the boundary. Scale bar: 10 μm .

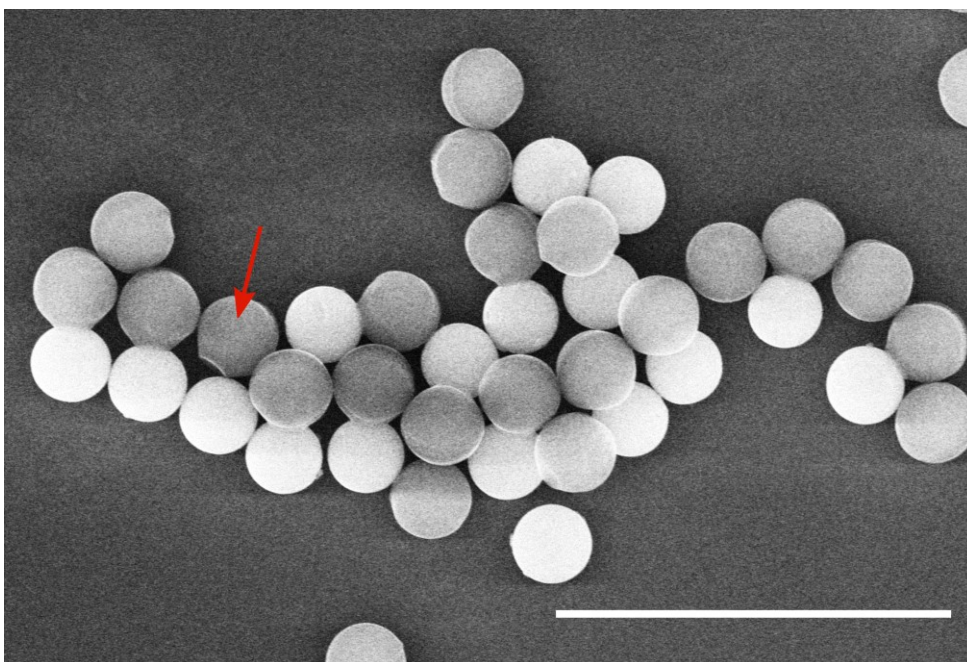


fig. S7. Harvesting of clusters at extremely low temperatures. SEM image showing broken PS and SiO₂ dumbbells (highlighted by the arrow) harvested at -196 °C. Rapid cooling causes cracking at the neck of the sintered clusters. The scale bars is 5 μm.

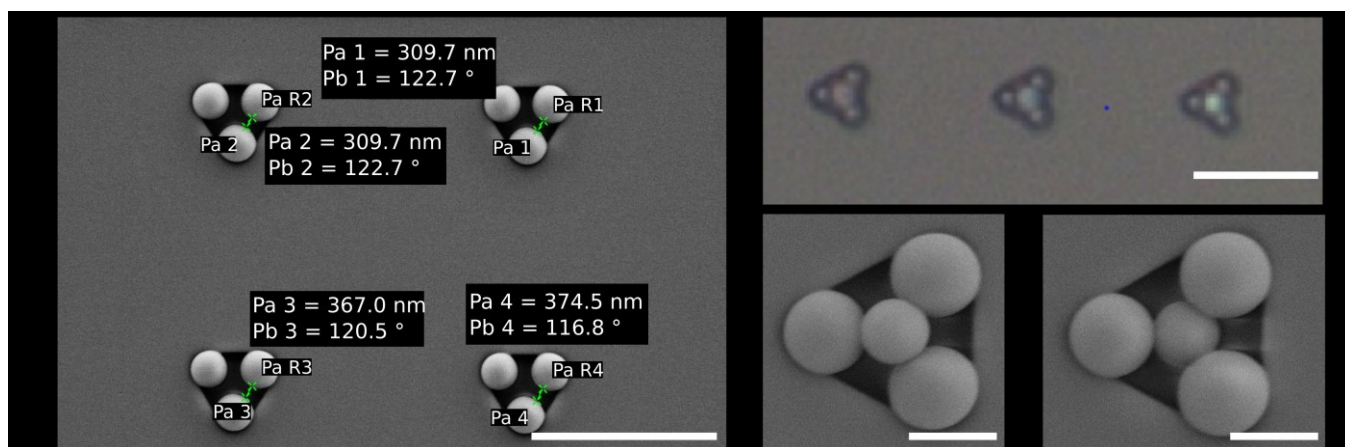


fig. S8. Effects of varying lateral trap dimensions on the structure of 3D clusters. (A) SEM image showing the variation in the space between the open trimers, mostly due to the variations in lateral trap dimensions. Scale bar: 5 μm . (B) Optical image showing the presence of a fourth particle on top of the trimers. Scale bar: 5 μm . (C and D) SEM images showing two different scenarios where the fourth particle sits at different heights. Scale bar: 1 μm . In some cases – due to variations in the trap size and the size distribution of the particles – the fourth particle might squeeze through the already assembled ones and end up on the bottom of the trap (D).

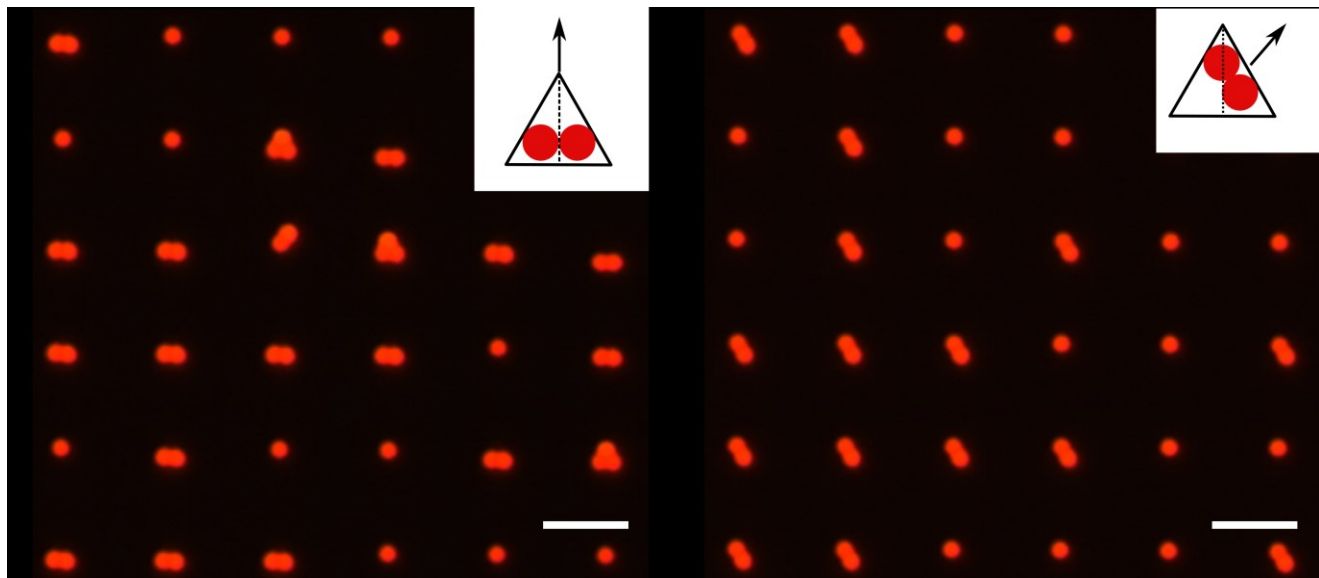


fig. S9. Effects of local assembly direction on the first sCAPA step of colloidal trimers. (A) Fluorescence micrograph of the deposited particles showing that when the local assembly direction is straight relative to the bisector of the predefined corner (inset), mostly two or three particles are assembled. (B) Fluorescence micrograph of the deposited particles showing that when the local assembly direction is shifted too much from the bisector (inset), often two particles may be assembled along the side of the trap, rather than only one particle in the corner. The scale bars are 5 μm .

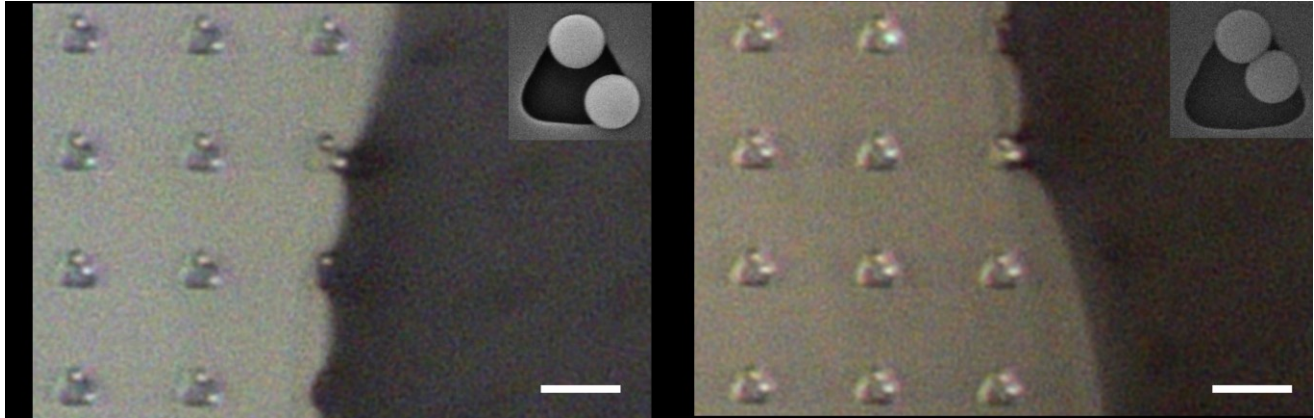


fig. S10. Effects of local assembly direction on the assembly of open colloidal trimers with three different lobes. (A) Optical micrograph showing that when the meniscus moves away from the occupied corner, a space is created between particles. Inset: SEM image of the two separated particles in the trap. **(B)** Optical micrograph showing that when the meniscus moves toward the occupied corner, the second particle is assembled in contact with the previously assembled one. Inset: SEM image of the two particles in contact in the trap. The scale bars are 5 μm .

Supplementary movies

Movie S1. The first assembly step for the fabrication of surfactant-like colloidal chains. The movie was captured at 15fps.

Movie S2. The second assembly step for the fabrication of surfactant-like colloidal chains. The movie was captured at 15fps.

Movie S3. Brownian motion of a dumbbell with a magnetic head and a PS lobe dispersed in water after harvesting. The movie was captured at 10 fps by mixing the fluorescence and transmission channels. The non-fluorescent magnetic SiO₂ particle appears dark and the fluorescent PS particle appears bright. The movie is three times faster than real time.

Movie S4. Brownian motion of a four-particle chain with a magnetic head and a PS tail dispersed in water after harvesting. The movie was captured at 10 fps by mixing the fluorescence and transmission channels. The non-fluorescent magnetic SiO₂ particle appears dark and the fluorescent PS particles appear bright. The movie is three times faster than real time.

Movie S5. Brownian motion of an eight-particle chain with a magnetic head and a PS tail dispersed in water after harvesting. The movie was captured at 10 fps by mixing the fluorescence and transmission channels. The non-fluorescent magnetic SiO₂ particle appears dark and the fluorescent PS particles appear bright. The movie is three times faster than real time.

Movie S6. Rotation of colloidal chains with a magnetic head in an external rotating magnetic field. The field rotation frequency is 1 Hz. The movie was captured at 100 fps by mixing the fluorescence and transmission channels. The non-fluorescent magnetic SiO₂ particle appears dark and the fluorescent PS particles appear bright.

Movie S7. Oscillation of colloidal chains with a magnetic head in an external oscillating magnetic field. The oscillation frequency is 0.5 Hz with a rotation amplitude of 270°. The movie was captured at 100 fps by mixing the fluorescence and transmission channels. The non-fluorescent magnetic SiO₂ particle appears dark and the fluorescent PS particles appear bright.

Movie S8. Translation of a colloidal chain with a magnetic head by a permanent magnet. The movie was captured at 10 fps by mixing the fluorescence and transmission channels. The non-fluorescent magnetic SiO₂ particle appears dark and the fluorescent PS particles appear bright.

Movie S9. The third assembly step for the fabrication of open PS trimers with three different lobes. The movie was captured at 6fps.